Journal of
Materials Chemistry A

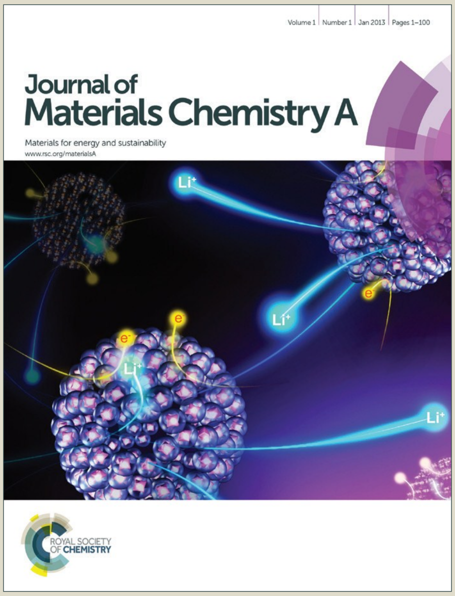

Volume 1 | Number 1 | Jan 2013 | Pages 1–100

Journal of
Materials Chemistry A

Materials for energy and sustainability
www.rsc.org/materialsA

ROYAL SOCIETY
OF CHEMISTRY

www.rsc.org/materialsA

Effective doping by spin-coating and enhanced thermoelectric power factors in SWCNT/P3HT hybrid films†

Cheon Taek Hong,‡[ab] Woohwa Lee,‡[a] Young Hun Kang,[a] Youngjae Yoo,[a] Juwhan Ryu,[b] Song Yun Cho*[a] and Kwang-Suk Jang*[a]

[a]*Division of Advanced Materials, Korea Research Institute of Chemical Technology, Daejeon 305-600, Republic of Korea. E-mail: kjang@krict.re.kr; scho@krict.re.kr*

[b]*Department of Polymer Science and Engineering, Chungnam National University, Daejeon 305-764, Republic of Korea*

†Electronic supplementary information (ESI) available: $\Delta V/\Delta T$ curve of the bar-coated SWCNT/P3HT hybrid film and photograph images of P3HT films.

‡These authors equally contributed.

Abstract

This study investigates a coating method for doping single-walled carbon nanotube (SWCNT)/poly(3-hexylthiophene) (P3HT) hybrid film. In the hybrid film, P3HT chains were very highly doped by simple spin-coating of a $FeCl_3$/nitromethane solution. Hybrid films doped by spin-coating exhibited power factors of 267 ± 38 μW $m^{-1}K^{-2}$, which is an improvement over that of hybrid films doped by conventional immersion, 103 ± 24 μW $m^{-1}K^{-2}$. The excellent thermoelectric performance is originated from the dramatically increased electrical conductivity by the sufficient doping of P3HT in the hybrid films.

Introduction

Thermoelectric materials are highly attractive as clean energy harvesting materials because they can turn waste heat into electricity. The performance of thermoelectric materials can be evaluated by measuring the Seebeck coefficient ($S = -\Delta V/\Delta T$, where ΔV is the voltage generated by a temperature difference ΔT within a thermoelectric material), electrical conductivity (σ), and thermal conductivity (κ). The thermoelectric performance is estimated using the dimensionless figure of merit ($ZT = S^2\sigma T/\kappa$). For high-performance thermoelectric generators, thermoelectric materials with a high Seebeck coefficient, high electrical conductivity, and low thermal conductivity should be used. If thermoelectric materials are processed as a thin film onto a substrate, the power factor ($S^2\sigma$) can be used as an alternative to the figure of merit. Although the 3ω method can be used for measuring the thermal conductivity of thermoelectric thin films, the measurement of the in-plane thermal conductivity is difficult due to thermal contact resistance, radiation loss, and heat conduction through the substrate.[1]

In recent years, thermoelectric conjugated polymers such as poly(3,4-ethylenedioxythiophene):poly(styrenesulfonate) (PEDOT:PSS) have been extensively studied because of their potential for light-weight, flexible, and low-cost printed thermoelectric generators.[2-11] However, there is still room for further improvement in the thermoelectric performance of conjugated polymers. Recently, it was found that single-walled carbon nanotubes (SWCNTs) are an effective filler for enhancing the thermoelectric performance of a conjugated polymer matrix.[12-14] Bounioux *et al.* reported that SWCNT/$FeCl_3$-doped poly(3-hexylthiophene) (P3HT) hybrid films exhibited power factors of 95 ± 12 μW $m^{-1}K^{-2}$ at room temperature.[12] Yu *et al*. reported that SWCNT/PEDOT:PSS/polyvinyl acetate (PVAc) hybrid films exhibited power factors up to 160 μW $m^{-1}K^{-2}$ at room temperature.[13] Yao *et al*. reported that SWCNT/camphorsulfonic acid (CSA)-doped polyaniline hybrid films exhibited power factors up to 176 μW $m^{-1}K^{-2}$ at room temperature.[14] Although these SWCNT/doped conjugated polymer hybrid films showed enhanced thermoelectric power factors, the performance still needs further improvement to reach the power factor of bismuth telluride (Bi_2Te_3) at room temperature, which is approximately 1000 μW $m^{-1}K^{-2}$.

This study examined a doping method using simple spin-coating that enhances the thermoelectric power factors of SWCNT/P3HT hybrid films. The SWCNT/P3HT hybrid films were prepared by a simple bar-coating process. The P3HT chains in a hybrid film were highly doped through spin-coating of a $FeCl_3$/nitromethane solution. These hybrid films exhibited power factors up to 308 μW $m^{-1}K^{-2}$, which is the highest value among inorganic/organic hybrid thermoelectric materials. For comparison, we also prepared SWCNT/P3HT hybrid films doped by the conventional immersion process. The hybrid film doped by immersion exhibited power factors up to 144 μW $m^{-1}K^{-2}$ at room temperature.

Results and discussion

Fig. 1 shows a schematic of the experimental procedure for the preparation of the SWCNT/ $FeCl_3$-doped P3HT hybrid film. For the ink formulation, P3HT (40 wt%) and SWCNTs (60 wt%) mixture in *o*-dichlorobenzene (*o*DCB) was sonicated in an ice bath. It is well-known that there is a strong π-π interaction between SWCNT and P3HT. This leads to the best dispersion of SWCNTs in a good solvent for P3HT, such as *o*DCB.[12,15,16] For the preparation of the SWCNT/P3HT hybrid film, the ink was bar-coated onto a glass substrate. The bar-coating process is advantageous for obtaining large-area uniform films, because the volume between the bar and the substrate can be precisely determined.[17-20] Because the undoped P3HT is not electrically conductive, doping of the hybrid films is required for their enhanced thermoelectric properties. To obtain SWCNT/highly doped P3HT hybrid films with a high electrical conductivity, in this study, 0.03 M $FeCl_3$/nitromethane solution was simply overcoated by spin-coating onto the as-prepared SWCNT/P3HT hybrid films. Additional rinsing and annealing are not required for the doping by spin-coating. In the case of conventional doping, the as-prepared hybrid films were immersed in the doping solution and rinsed with methanol.

The thickness of the as-prepared SWCNT/P3HT hybrid film was 55.1 ± 6.2 nm (Fig. 2a). After doping by immersion and spin-coating, the thicknesses of the SWCNT/ $FeCl_3$-doped P3HT hybrid films were 51.2 ± 3.0 nm and 49.7 ± 2.6 nm, respectively (Fig. 2a). Although the film thicknesses were slightly decreased after the doping processes, the differences were within the standard deviation. The Seebeck coefficients of the hybrid films were measured under dark ambient conditions utilizing a custom built system (Fig. 2b). The Seebeck coefficient was estimated from a slope of the straight line fit of $\Delta V/\Delta T$ (Fig. S1). The hybrid films exhibited positive values of Seebeck coefficient, because both SWCNTs and P3HT have p-type characteristics. To estimate the thermoelectric properties of the bar-coated hybrid films, electrical conductivity and power factor were also measured (Fig. 2c and 2d). The trade-off relationship between the Seebeck coefficient and electrical conductivity of doped conjugated polymers is well-known.[5,21-26] As the doping level of conjugated polymers increases, the Seebeck coefficient decreases and the electrical conductivity increases. The typical behavior of conjugated polymers was also observed in the SWCNT/P3HT hybrid films. After the conventional doping of the as-prepared SWCNT/P3HT hybrid films, the Seebeck coefficient decreased from 56.1 ± 2.3 μV K^{-1} to 40.0 ± 3.1 μV K^{-1}, and the electrical conductivity increased from 141 ± 13 S cm^{-1} to 638 ± 57 S cm^{-1}. After doping by spin-coating, the change in thermoelectric properties was even more significant. The Seebeck coefficient and electrical conductivity of the hybrid films doped by spin-coating were 31.1 ± 2.1 μV K^{-1} and 2760 ± 170 S cm^{-1}, respectively. From the Seebeck coefficient and electrical conductivity, the power factors of the hybrid films were calculated. The power factors of the SWCNT/P3HT hybrid films undoped, doped by immersion, and doped by spin-coating were 44.4 ± 6.1 μW $m^{-1}K^{-2}$, 103 ± 24 μW $m^{-1}K^{-2}$, and 267 ± 38 μW $m^{-1}K^{-2}$, respectively. Using both doping processes, the power factors of the hybrid films increased. The increased power factors are thought to be due to the increased electrical conductivities. Using the spin-coating doping process, the electrical conductivity and power factor of the hybrid films increased more dramatically. The maximum power factor of the SWCNT/P3HT hybrid film doped by spin-coating reached 308 μW $m^{-1}K^{-2}$. To the best of our knowledge, this is the highest value among inorganic/organic hybrid thermoelectric materials.

Fig. 3 shows the scanning electron microscope (SEM) images of the SWCNT/P3HT hybrid films undoped, doped by immersion, and doped by spin-coating. In the hybrid films, the networks of SWCNT bundles are clear. The interconnected networks of SWCNT bundles are also observed in the atomic force microscope (AFM) images (Fig. 4). The inter-SWCNT bundle connections are thought to be the electrical pathways in the hybrid thin films. In all three films, the diameters of 1-dimensional SWCNT bundles were in the range of 10–30 nm. After both doping processes, surface morphologies of the hybrid films were maintained. It has been reported that the thicknesses and morphologies of the P3HT films significantly affect the thermoelectric properties.[20] However, this study did not find meaningful differences in thicknesses and surface morphologies among the hybrid films undoped, doped by immersion, and doped by spin-coating. Because of the inter-SWCNT bundle connections, an acceptable electrical conductivity of 141 ± 13 S cm^{-1} was measured, even in the SWCNT/non-conductive P3HT hybrid films. After the effective doping of P3HT chains by spin-coating, the electrical conductivity of the hybrid films increased to 2760 ± 170 S cm^{-1}, which is comparable to that of indium tin oxide (ITO) electrodes.

Fig. 5 shows the UV-vis spectra of the SWCNT/P3HT hybrid films undoped, doped by immersion, and doped by spin-coating. The relative doping level of P3HT can be estimated with the change in its absorbance.[26-29] The decrease in the absorbance for the neutral form (λ_{max} = 560 nm) and increase in the absorbance for the oxidized form (λ_{max} = 800 nm) are evidence of the dopant uptake.[28,29] During the doping process, dopants diffuse into the P3HT chains and capture electrons from the P3HT chains. The absorbance at 560 nm decreased more in the hybrid film doped by spin-coating than in the hybrid film doped by immersion. (The absorbance peak at 800 nm could not be extracted from the absorbance for SWCNTs.)

The electrical conductivity of P3HT can increase greatly by doping, whereas SWCNTs are insensitive to doping. The increased electrical conductivity of SWCNT/P3HT hybrid films doped by spin-coating is thought to be originated from sufficient doping of P3HT matrix. It has been reported that the doping method significantly affects the electrical conductivity and the power factor of conjugated polymers.[30,31] Drastic enhancement of the electrical conductivities of SWCNT/conjugate polymer hybrids by improving the electrical conductivities of the polymer matrices have also been reported.[12,32] To estimate the influence of the doping method on the electrical properties of P3HT matrix, we prepared 50 nm-thick P3HT films that were undoped, doped by immersion, and doped by spin-coating (Fig. S2). The electrical conductivities of P3HT films undoped, doped by immersion, and doped by spin-coating were ~10^{-5} S cm^{-1}, ~10^{-4} S cm^{-1}, and 61.9 ± 7.6 S cm^{-1}, respectively. To estimate the relative doping levels, UV-vis spectra of the 50 nm-thick P3HT films undoped, doped by immersion, and doped by spin-coating were obtained (Fig. 6). Highly doped state of the P3HT film after doping by spin-coating is confirmed by the largely decreased absorbance at 560 nm and greatly increased absorbance at 800 nm. In the spectrum of the P3HT film doped by immersion and rinsed with methanol, the changes in the absorbance are smaller. The doping levels of the P3HT films were obtained from elemental concentrations of S and Cl, measured by energy dispersed X-ray spectroscopy (EDS) measurements.[28,29] The doping levels of P3HT films doped by immersion and doped by spin-coating were 0.19 and 0.48, respectively. The doping level of 0.48 is comparable to that of the heavily doped P3HT films (0.4).[28,29] The UV-vis spectra and EDS measurements correspond well to the measured electrical conductivities. The insufficiently doped state of the P3HT film after doping by immersion is might be due to dedoping during rinsing. Previously, we have reported that the lower thickness of P3HT films results in a relatively greater extent of dedoping during the rinsing process after conventional doping by immersion.[20] For example, the electrical conductivity of the 200 nm-thick P3HT film doped by immersion and rinsed with methanol was less than 10^{-3} S cm^{-1}. To verify this, we prepared the P3HT film doped by immersion and not rinsed, whose highly doped state was confirmed by UV-vis spectroscopy (Fig. 6). Unfortunately, the electrical conductivity and elemental concentrations of this P3HT film could not be measured because of irregular deposition of the excess dopants on the film surface (Fig. S2). In case of doping by spin-coating, the residual solution with excess dopants and reaction products such as Fe^{2+} and Cl^{-} ions are removed from the film surface by the spinning process and additional rinsing is not required. Although the aggregated excess dopants and reaction products on the film surface were not observed, they might still be remaining present. It seems that the amount of the impurities is negligible to obtain reliable thermoelectric performances in this study. However, the effect of the impurities remaining on the film surface on the electrical properties cannot be completely excluded.

Kymakis and Amaratunga reported that the electrical conduction in SWCNT films follows a three-dimensional variable-range hopping model, while that in SWCNT/non-conductive polymer hybrid films obeys a fluctuation-induced tunneling model.[33] In the hybrid films, the non-conductive polymer matrix acts as a barrier to bundle-to-bundle hopping. Because the axial electrical conductivity of SWCNT bundles is known to be 10000 – 30000 S cm^{-1},[34] the resistance between the SWCNT bundles is a dominant factor determining the total electrical conductivity of the SWCNT/P3HT hybrid films.[12] The inter-SWCNT bundle resistance in the hybrid film could be reduced by decreasing the average inter-bundle distance and/or by increasing the electrical conductivity of the polymer matrix. This was confirmed experimentally for the SWCNT/P3HT hybrid films (Fig. 7). We measured electrical conductivities of the SWCNT/P3HT hybrid films undoped, doped by immersion, and doped by spin-coating, as a function of the SWCNT composition. The electrical conductivities of all three types of hybrid films increased with increasing SWCNT composition. The average inter-bundle distance should decrease with increasing SWCNT composition. In the SWCNT composition range 20 - 60 wt%, the electrical conductivities of the SWCNT/P3HT hybrid films increased dramatically after doping by spin-coating, whereas the electrical conductivity enhancement of the hybrid films doped by immersion was relatively less. Doping by spin-coating increases the electrical conductivity of the P3HT film from ~10^{-5} S cm^{-1} to 61.9 ± 7.6 S cm^{-1}. In the SWCNT/P3HT hybrid film doped by spin-coating, the increased electrical conductivity of the P3HT matrix could lower the resistance between the SWCNT bundles. It can be concluded that doping by spin-coating is more effective to obtain highly doped P3HT in the hybrid films than conventional doping by immersion. It is suggested that the increased electrical conductivity and power factor of the hybrid films doped by spin-coating are due to the sufficient doping of P3HT in the hybrid films. The results of this study indicate that the doping method affects the thermoelectric properties of conjugated polymer-based composites. Through effective doping, thermoelectric power factor of conjugated polymer-based composites could be enhanced.

Conclusion

In summary, SWCNT/P3HT hybrid thin films were prepared by simple bar-coating. Within the hybrid films, SWCNT bundles with diameters in the range of 10–30 nm formed an interconnected network. The Seebeck coefficient, electrical conductivity, and power factor of the as-prepared SWCNT/P3HT hybrid films were 56.1 ± 2.3 μV K^{-1}, 141 ± 13 S cm^{-1}, and 44.4 ± 6.1 μW $m^{-1}K^{-2}$, respectively. The thermoelectric properties of the hybrid films were shown to be greatly enhanced by doping *via* spin-coating process. After doping by spin-coating with an $FeCl_3$/nitromethane solution, the Seebeck coefficient, electrical conductivity, and power factor of the hybrid films were 31.1 ± 2.1 μV K^{-1}, 2760 ± 170 S cm^{-1}, and 267 ± 38 μW $m^{-1}K^{-2}$, respectively. This study suggests that SWCNT/highly doped conjugated polymer hybrid films may be promising candidates for room temperature thermoelectric applications.

Experimental

Preparation of SWCNT/P3HT hybrid films

Purified HiPco single-walled carbon nanotubes were purchased from Unidym. Regioregular P3HT (M_w 37,685 g mol^{-1}, regioregularity 98.5%), anhydrous ferric chloride, and nitromethane were purchased from Sigma-Aldrich. *o*DCB was purchased from Junsei. All chemicals in this study were used as received. The P3HT was dissolved in *o*DCB. The SWCNTs were then added to this solution. The mixture was sonicated in an ice bath using a probe sonicator (VCX-750 Vibra-Cell, Sonics & Materials) at 10 W for 1 hr. This ink was then bar-coated onto a glass substrate (76 mm × 26 mm). During the bar-coating process, 6.35 mm diameter bar closely wound with a 32 µm diameter wire was used and the carrying speed of the bar was maintained at 10 mm/s during the bar-coating process. For conventional doping, the as-prepared SWCNT/P3HT films were doped by immersion in 0.03 M $FeCl_3$/nitromethane solution for 1 hr. The doped P3HT films were finally rinsed with methanol to remove excess dopants. For doping by spin-coating, 0.03 M $FeCl_3$/nitromethane solution was spin-coated at 3000 rpm for 30 s onto the as-prepared SWCNT/P3HT films.

Characterizations

The Seebeck coefficients of the hybrid films were measured under dark ambient conditions utilizing a custom built system. Before the measurement, silver paste was printed onto the SWCNT/P3HT hybrid films through a screen mask. Two silver electrodes, 5 mm in width, were separated by a distance of 40 mm. The temperature gradient between the two electrodes was varied from 1 to 10 °C. The Seebeck voltage generated by the temperature difference was measured with a Keithley 2182A Nanovoltmeter. The Seebeck coefficient was estimated from a slope of the straight line fit of $\Delta V/\Delta T$ (Fig. S1). The electrical conductivity of the SWCNT/P3HT hybrid films was measured with the standard van der Pauwe direct current four-probe method.[35] All the measurements were conducted at room temperature using a Keithley 195A digital multimeter and a Keithley 220 programmable current source. The thickness of the films was determined with an alpha-step surface profiler (α-step DC50, KLA Tencor). UV-vis spectra of the hybrid films were recorded with a Scinco UV S-2100. The surface morphologies of the films were observed with a field-emission SEM (MIRA3, TESCAN) operating at 20 kV and a tapping-mode AFM (Nanoscope IV, Digital Instruments).

Acknowledgements

This work was supported by a grant from the R&D Convergence Program of NST (National Research Council of Science & Technology), a grant from the KRICT Core Project (KK-1507-C6), and the Center for Advanced Soft-Electronics funded by the Ministry of Science, ICT and Future Planning as Global Frontier Project (2011-0031628).

Notes and references

1 A. Weathers, Z. U. Khan, R. Brooke, D. Evans, M. T. Pettes, J. W. Anderson, X. Crispin and L. Shi, *Adv. Mater.*, 2015, **27**, 2101.

2 M. He, F. Qiu and Z. Lin, *Energy Environ. Sci.*, 2013, **6**, 1352.

3 M. Chanbinyc, *Nat. Mater.*, 2014, **13**, 119.

4 Y. Sun, P. Sheng, C. Di, F. Jiao, W. Xu, D. Qiu and D. Zhu, *Adv. Mater.*, 2012, **24**, 932.

5 O. Bubnova, Z. U. Khan, A. Malti, S. Braun, M. Fahlman, M. Berggren and X. Crispin, *Nat. Mater.*, 2011, **10**, 429.

6 G-H. Kim, L. Shao, K. Zhang and K. P. pipe, *Nat. Mater.*, 2013, **12**, 719.

7 T. Park, C. Park, B. Kim, H. Shin and E. Kim, *Energy Environ. Sci.*, 2013, **6**, 788

8 S. H. Lee, H. Park, S. Kim, W. Son, I. W. Cheong and J. H. Kim, *J. Mater. Chem. A*, 2014, **2**, 7288.

9 M. Culebras, C. M. Gómez and A. Cantarero, *J. Mater. Chem. A*, 2014, **2**, 10109.

10 Q. Zhang, Y. Sun, W. Xu and D. Zhu, *Energy Environ. Sci.*, 2012, **5**, 9639.

11 M. He, J. Ge, Z. Lin, X. Feng, X. Wang, H. Lu, Y. Yang and F. Qiu, *Energy Environ. Sci.*, 2012, **5**, 8351.

12 C. Bounioux, P. Díaz-Chao, M. Campoy-Quiles, M. S. Martín-González, A. R. Goñi, R. Yerushalmi-Rozen and C. Müller, *Energy Environ. Sci.*, 2013, **6**, 918.

13 C. Yu, K. Choi, L. Yin and J. C. Grunlan, *ACS Nano*, 2011, **5**, 7885.

14 Q. Yao, Q. Wang, L. Wang and L. Chen, *Energy Environ. Sci.*, 2014, **7**, 3801.

15 S. Ren, M. Bernardi, R. R. Lunt, V. Bulovic, J. C. Grossman and S. Gradečak, *Nano Lett.*, 2011, **11**, 5316.

16 J. Zou, L. Liu, H. Chen, S. I. Khondaker, R. D. McCullough, Q. Huo and L. Zhai, *Adv. Mater.*, 2008, **20**, 2055.

17 J. Ouyang, T.-F. Guo, Y. Yang, H. Higuchi, M. Yoshioka and T. Nagatsuka, *Adv. Mater.*, 2002, **14**, 915.

18 D. Khim, H. Han, K.-J. Baeg, J. Kim, S.-W. Kwak, D.-Y. Kim and Y.-Y. Noh, *Adv. Mater.*, 2013, **25**, 4302.

19 *Coatings Technology Handbook*, ed. A. A. Tracton, CRC Press, Boca Raton, 2006

20 C. T. Hong, Y. Yoo, Y. H. Kang, J. Ryu, S. Y. Cho and K.-S. Jang, *RSC Adv.*, 2015, **5**, 11385.

21 Y. Xuan, X. Liu, S. Desbief, M. Fahlman, R. Lazzaroni, M. Berggren, J. Cornil, D. Emin and X. Crispin, *Phys. Rev. B*, 2010, **82**, 115454.

22 R. B. Aïch, N. Blouin, A. Bouchard, M. Leclerc, *Chem. Mater.*, 2009, **21**, 751.

23 T. O. Poehler and H. E. Katz, *Energy Environ. Sci.*, 2012, **5**, 8110.

24 O. Bubnova, Z. U. Khan, H. Wang, S. Braun, D. R. Evans, M. Fabretto, P. Hojati-TAlemi, D. Dagnelund, J.-B. Arlin, Y. H. Geerts, S. Desbief, D. W. Breiby, J. W. Andreasen, R. Lazzaroni, W. M. Chen, I. Zozoulenko, M. Fahlman, P. J. Murphy, M. Berggren and X. Crispin, *Nat. Mater.*, 2014, **13**, 190.

25 Q. Zhang, Y. Sun, W. Xu and D. Zhu, *Adv. Mater.*, 2014, **26**, 6829.

26 Q. Zhang, Y. Sun, W. Xu and D. Zhu, *Macromolecules*, 2014, **47**, 609.

27 T.-C. Chung, J. H. Kaufman, A. J. Heeger and F. Wudl, *Phys. Rev. B*, 1984, **30**, 702.

28 B. Endrődi, J. Mellár, Z. Gingl, C. Visy and J. Janáky, *RSC Adv.*, 2014, **4**, 55328.

29 B. Endrődi, J. Mellár, Z. Gingl, C. Visy and J. Janáky, *J. Phys. Chem. C*, 2015, DOI: 10.1021/acs.jpcc.5b00135.

30 A. M. Glaudell, J. E. Cochran, S. N. Patel and M. L. Chabinyc, *Adv. Energy Mater.*, 2015, **5**, 1401072.

31 R. A. Schlitz, F. G. Brunetti, A. M. Gludell, P. L. Miller, M. A. Brady, C. J. Takacs, C. J. Hawker and M. L. Chabinyc, *Adv. Mater.*, 2014, **26**, 2825.

32 R. Allen, L. Pan, G. G. Fuller and Z. Bao, *Appl. Mater. Interfaces*, 2014, **6**, 9966.

33 E. Kymakis and G. A. J. Amaratunga, *J. Appl. Phys.*, 2006, **99**, 084302.

34 A. Thess, R. Lee, R. Nikolaev, H. Dai, P. Petit, J. Robert, C. Xu, Y. H. Lee, S. G. Kim, A. G. Rinzler, D. T. Colbert, G. E. Scuseria, D. Tománek, J. E. Fischer, R. E. Smalley, *Science*, 1958, **273**, 483.

35 L. T. van der Pauwe, *Philips Res. Rep.*, 1958, **13**, 1.

Figures

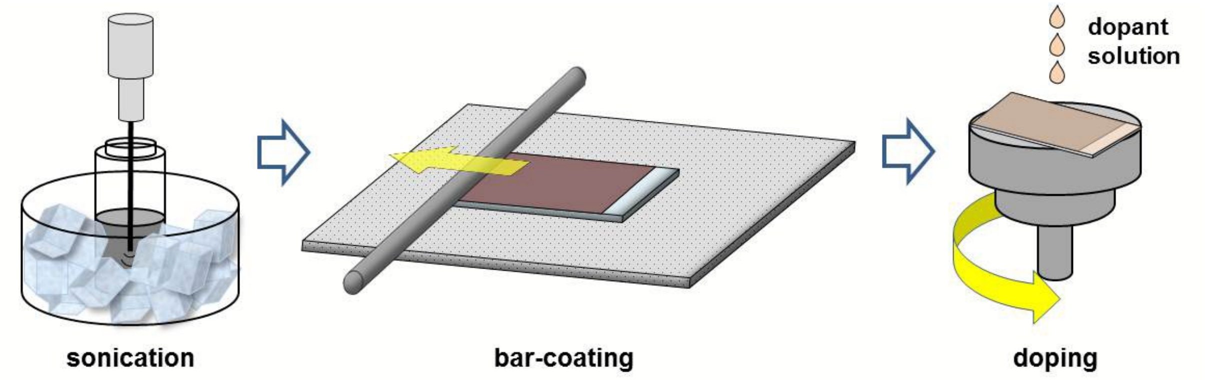

Fig. 1 Schematic diagram of the fabrication and doping processes of the bar-coated SWCNT/P3HT hybrid film.

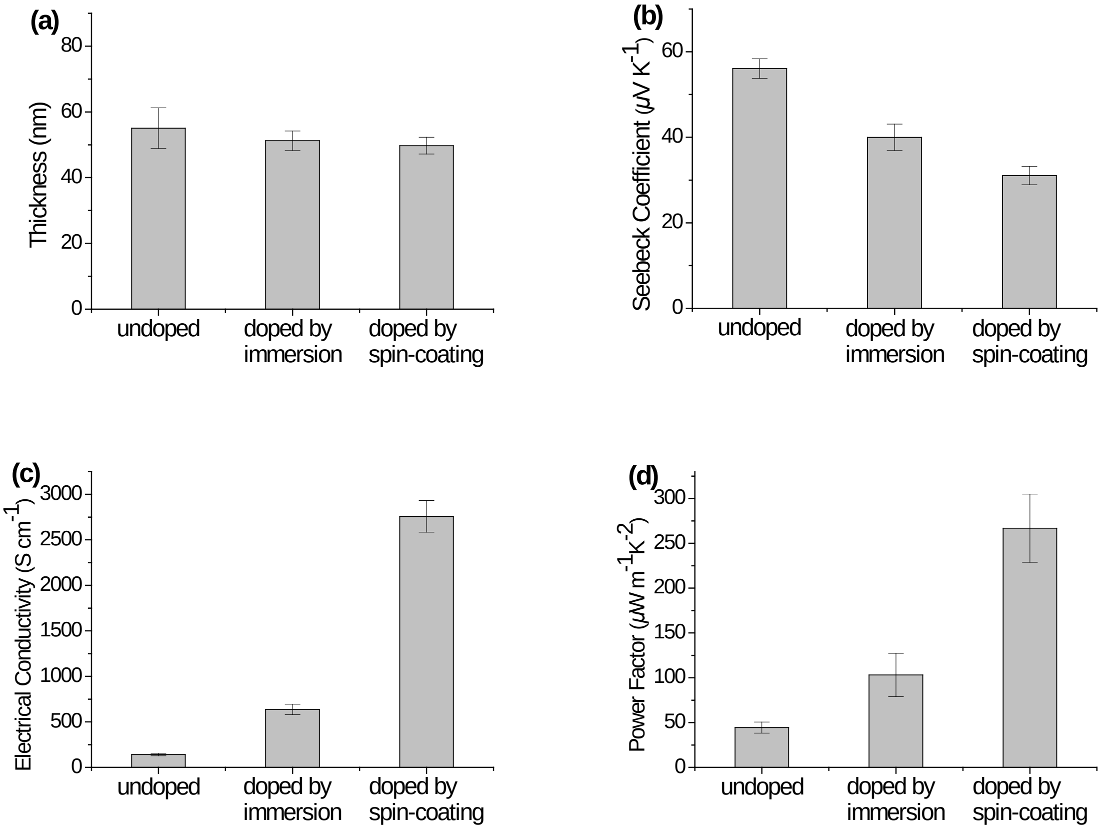

Fig. 2 (a) Thicknesses, (b) Seebeck coefficients, (c) electrical conductivities, and (d) power factors of the bar-coated SWCNT/P3HT hybrid films undoped, doped by immersion, and doped by spin-coating, respectively.

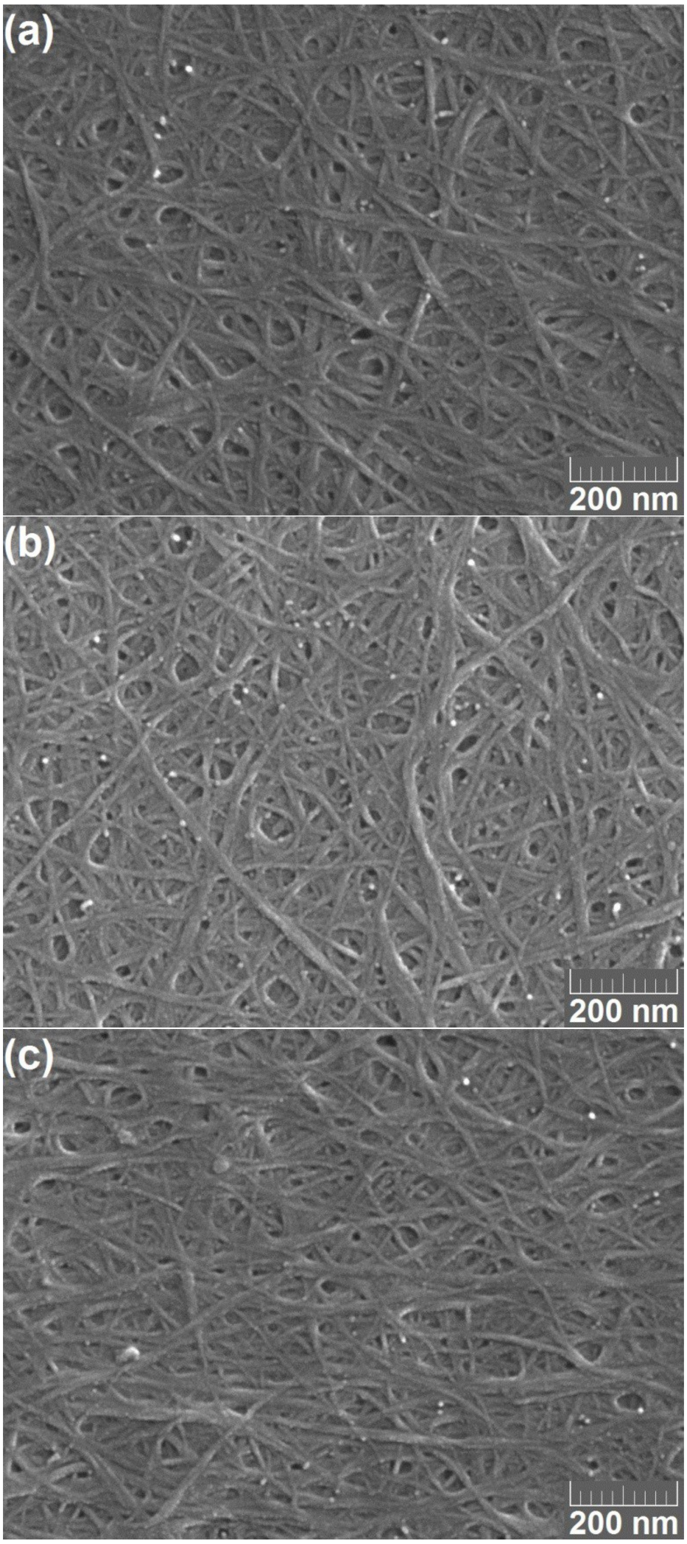

Fig. 3 SEM images of the bar-coated SWCNT/P3HT hybrid films (a) undoped, (b) doped by immersion, and (c) doped by spin-coating.

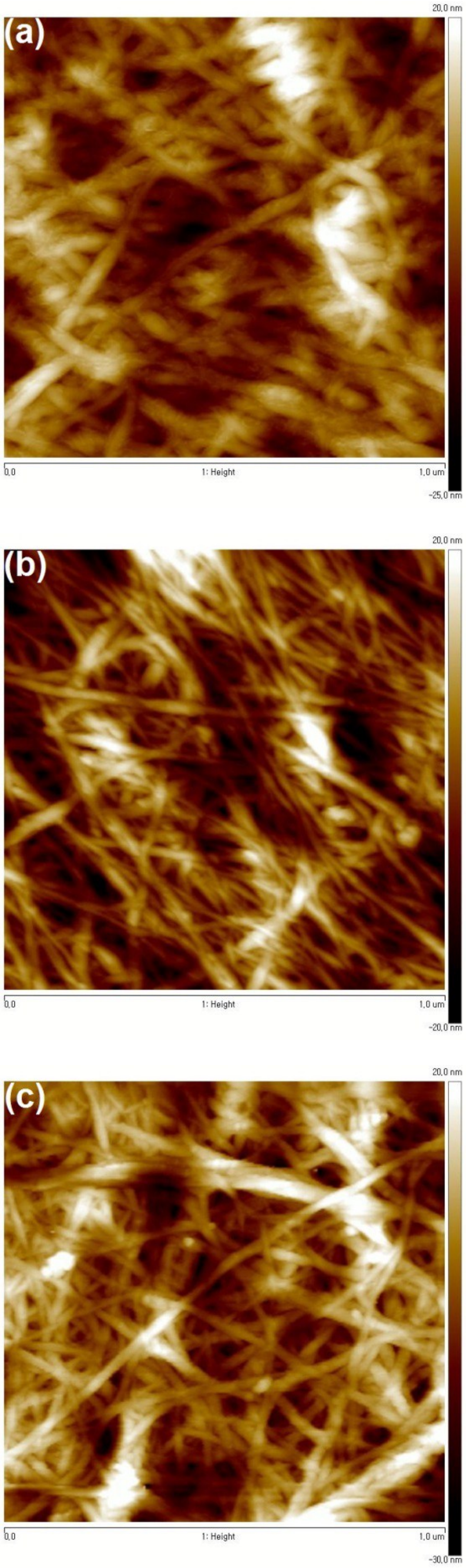

Fig. 4 AFM images (1 μm × 1 μm) of the bar-coated SWCNT/P3HT hybrid films (a) undoped, (b) doped by immersion, and (c) doped by spin-coating.

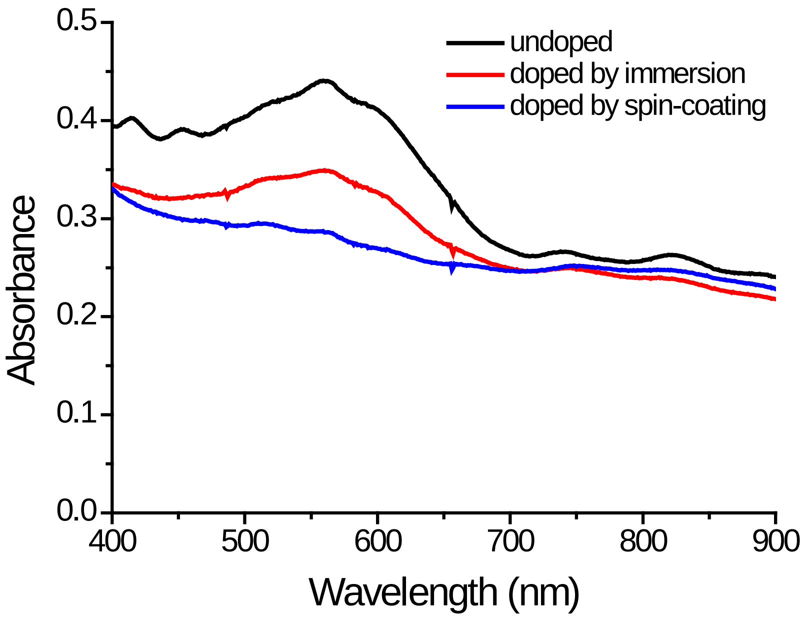

Fig. 5 UV-vis spectra of the bar-coated SWCNT/P3HT hybrid films undoped, doped by immersion, and doped by spin-coating.

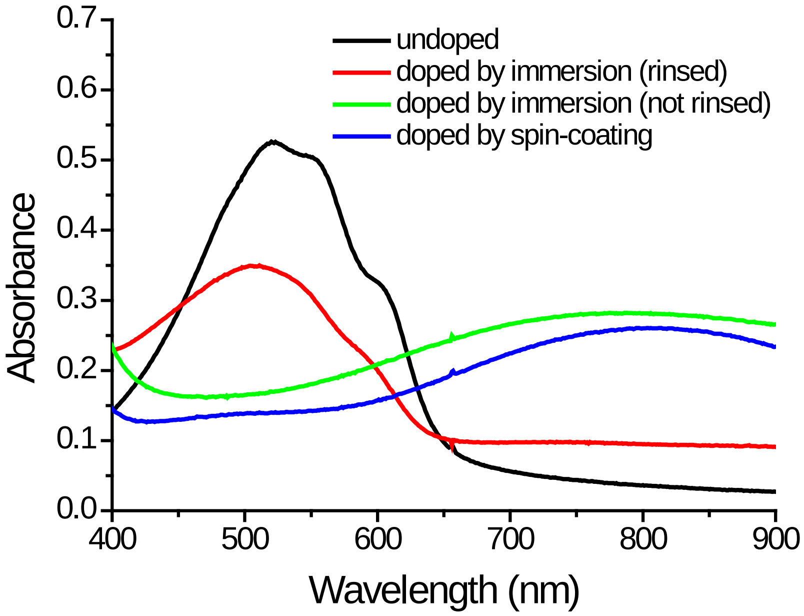

Fig. 6 UV-vis spectra of the P3HT films undoped, doped by immersion, and doped by spin-coating.

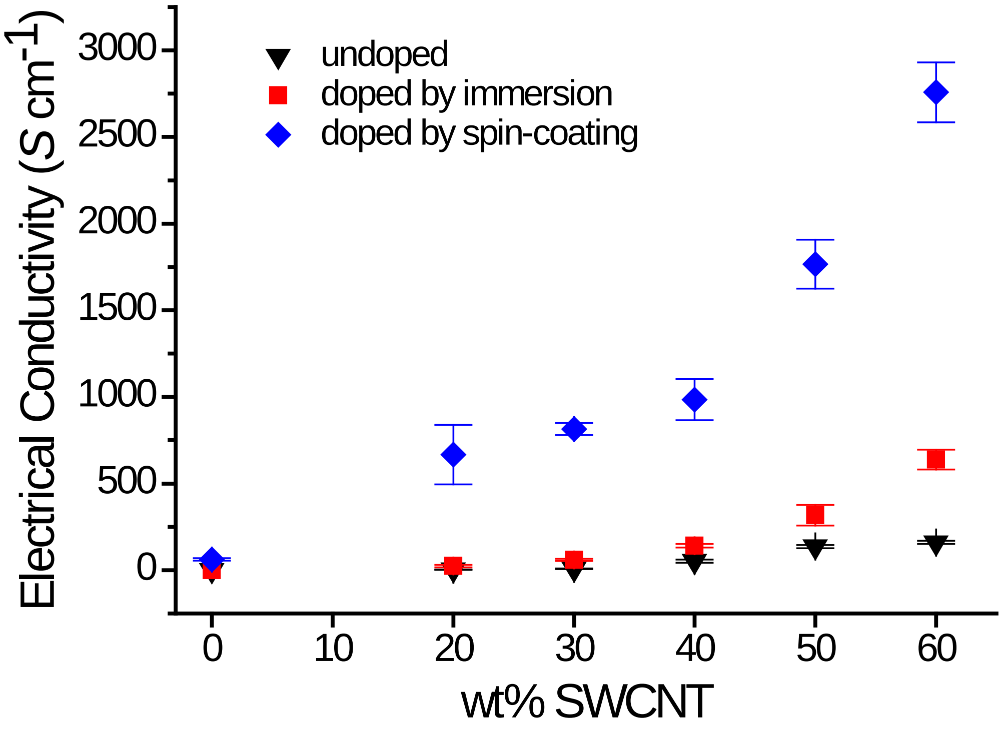

Fig. 7 Electrical conductivities of the SWCNT/P3HT hybrid films undoped, doped by immersion, and doped by spin-coating, as a function of the SWCNT composition.

The single-walled carbon nanotube (SWCNT)/poly(3-hexylthiophene) (P3HT) hybrid films doped by spin-coating exhibited power factors up to 308 μW $m^{-1}K^{-2}$.